EUROPEAN ORGANIZATION FOR NUCLEAR RESEARCH

CERN-EP/2001-072
October 4, 2001

Measurement of the charged-particle multiplicity and inclusive momentum distributions in Z decays at LEP

The L3 Collaboration

Abstract

The charged-particle multiplicity distribution and the inclusive momentum distribution, in terms of the variable ξ, are measured for all hadronic events as well as for light-quark and b-quark events in e^+e^- collisions at the Z pole. Moments of the charged-particle multiplicity distributions are calculated, and the peak positions of the ξ distributions determined.

The multiplicity distributions are studied in terms of their H_q moments. Their quasi-oscillations when plotted versus the rank of the moment are compared with different theoretical approaches.

Submitted to *Phys. Lett. B*

Introduction

Since quarks and gluons are not observed directly, the understanding of the hadronization process whereby a quark-gluon system evolves to hadrons is of importance and provides a tool for studying the quark-gluon system itself. Two of the most basic characteristics of the resulting hadronic system are the number of hadrons produced and their momentum distribution.

Assuming local parton-hadron duality (LPHD) [1], characteristics of both the charged-particle multiplicity distribution and the single-particle inclusive momentum distribution, which we study in terms of the variable $\xi = \ln(\sqrt{s}/2p)$, where p is the momentum of a particle and $\sqrt{s}$ is the center-of-mass energy, are directly related to the characteristics of the corresponding parton distributions. The parton distributions are calculable using perturbative quantum chromo-dynamics (pQCD). In particular, the dependences on $\sqrt{s}$ of the mean of the charged-particle multiplicity distribution, $\langle n \rangle$, and of the peak position of the ξ distribution, ξ^*, are important tests of pQCD. Since the flavor composition of the quarks produced in e^+e^- interactions changes with $\sqrt{s}$, understanding of the energy dependence requires a flavor decomposition. In this paper, results are presented on the charged-particle multiplicity and inclusive momentum distributions for hadronic decays of the Z boson, for b- and for light-quark (u, d, s or c) events as well as for all events.

The charged particle multiplicity is a fundamental tool in the study of particle production. Independent emission of single particles leads to a Poissonian multiplicity distribution. Deviations from this shape, therefore, reveal correlations [2]. To study the shape we use the normalized factorial moments. In terms of the multiplicity distribution, $P(n)$, the normalized factorial moment of rank q is defined by

$$F_q = \frac{\sum_{n=q}^{\infty} n(n-1)...(n-q+1)P(n)}{(\sum_{n=1}^{\infty} nP(n))^q} \quad . \tag{1}$$

The factorial moment of rank q corresponds to an integral over the q-particle density and reflects correlations in the production of up to q particles. If the particle distribution is Poissonian, all F_q are equal to one. If the particles are correlated, the distribution is broader and the F_q are greater than unity. If the particles are anti-correlated, the distribution is narrower and the F_q are less than unity.

Normalized cumulant factorial moments, K_q, are obtained from the normalized factorial moments by

$$K_q = F_q - \sum_{m=1}^{q-1} \frac{(q-1)!}{m!\,(q-m-1)!}\, K_{q-m} F_m \quad . \tag{2}$$

These K_q correspond to the phase-space integral over the q-particle correlation function which describes the genuine correlations between q particles, *i.e.*, q-particle correlations which are not a consequence of correlations among fewer than q particles.

Since $|K_q|$ and F_q both increase rapidly with q, it is useful to define the H_q moments,

$$H_q = \frac{K_q}{F_q} \quad , \tag{3}$$

which have the same order of magnitude over a large range of q.

The shape of the charged-particle multiplicity distribution analyzed in terms of the H_q has been found to reveal quasi-oscillations [3, 4], when plotted versus the rank q, in e^+e^-, as well as hadron-hadron, hadron-ion and ion-ion interactions.

This result in e^+e^- annihilation is usually interpreted in terms of pQCD, which provides us with calculations of the H_q of the parton multiplicity distribution [3, 5]. The expected behavior of H_q *vs.* q is quite sensitive to the approximation used, as is illustrated qualitatively in Figure 1 for the double leading logarithm approximation (DLLA), the modified leading logarithm approximation (MLLA), the next-to-leading logarithm approximation (NLLA), and the next-to-next-to-leading logarithm approximation (NNLLA). In the NNLLA a negative first minimum is expected near $q = 5$ and quasi-oscillations about zero are expected for larger values of q.

The LPHD hypothesis assumes that the hadronization does not distort the shape of the multiplicity distribution. If this is valid, the same behavior may be expected for the charged-particle multiplicity distribution as for the parton multiplicity distribution.

In addition to the charged-particle multiplicity distribution, we also measure jet multiplicity distributions and their moments obtained for a large range of values of the jet resolution parameter, $y_{\rm cut}$. Since jets obtained for energy scales above 1–2 GeV fall into the domain of validity of pQCD, they should correspond closely to the underlying partons. This allows a more direct test of pQCD, minimizing assumptions, such as LPHD, concerning the evolution of partons into hadrons.

The behavior of the H_q can also be interpreted in a more phenomenological way. Although the negative binomial distribution*) (NBD) describes the charged-particle multiplicity distribution in various types of interactions [6], it is less successful for hadronic Z decays [7]. The existence of H_q oscillations further contradicts the NBD description, which can be shown analytically not to have oscillations. On the other hand, oscillations can occur for a sum of NBDs, which may be plausible if we view the complete event sample as a mixture of different types of event, *e.g.*, 2-jet and 3-jet events [8] or light- and b-quark events [9]. The charged-particle multiplicity distribution is then the weighted average of the distributions of the different types of event. For example, in terms of 2- and 3-jet events the multiplicity distribution is then given by

$$P_{\rm 2NB}(n) = R_2\, P_{\rm NB}(n;\mu_2,k_2) + (1-R_2)\, P_{\rm NB}(n;\mu_3,k_3) \tag{4}$$

where R_2 is the fraction of events in the 2-jet sample, and μ_i and k_i are determined from the experimental charged-particle multiplicity distribution of that type of event.

Experimental procedures

Event selection

This analysis is based on 1.5 million hadronic events collected by the L3 detector [10] at LEP in the years 1994 and 1995 at the Z pole.

Events are selected in a two-step procedure [11]. First, at least 15 calorimetric clusters of at least 100 MeV are required in order to reduce background from the $e^+e^- \to \tau^+\tau^-$ process. Hadronic events are then selected by requiring small energy imbalance both along and transverse to the beam direction.

The second step is the selection of charged tracks measured in the central tracker and the silicon micro-vertex detector. A number of quality cuts are used to select well-measured tracks.

*) $P_{\rm NB}(n;\mu,k) = \frac{\Gamma(k+n)}{\Gamma(n+1)\Gamma(k)} \left(\frac{k}{\mu+k}\right)^k \left(\frac{\mu}{\mu+k}\right)^n$, where μ is the mean and k is related to the dispersion, D, by $k = 1/(D^2/\mu^2 - 1/\mu)$.

Further, the thrust direction calculated from the charged tracks is required to lie within the full acceptance of the central tracker. The track selection efficiency, determined from Monte Carlo, is about 75%. The resulting data sample corresponds to approximately one million selected hadronic events, and has a purity greater than 99%.

To correct for detector acceptances and inefficiencies, we make use of the JETSET 7.4 [12] parton shower Monte Carlo program, tuned using L3 data. Events are generated, passed through the L3 detector simulation program [13], and further subjected to time-dependent detector effects. Then they are reconstructed and the events and tracks are selected in the same way as the data. For systematic studies we also use events generated by ARIADNE 4.2 [14]. For comparison with the results, we use HERWIG 5.9 [15] as well as JETSET.

To select b- and light-quark enhanced samples, we use the full three-dimensional information on tracks from the central tracker to calculate for each track the probability that it originated at the primary vertex [16]. We select b- and light-quark samples with purities of about 96% and 93% and efficiencies of about 38% and 96%, respectively.

Unfolding

The resulting multiplicity and ξ distributions are fully corrected for detector resolution using an iterative Bayesian unfolding method [17]. For the multiplicity distribution this works as follows. The detector and generator level Monte Carlo events are used to construct a matrix $R(n_{\rm det}, n)$ which represents the probability that $n_{\rm det}$ tracks would be detected if n charged particles were produced. A distribution, $P_0(n)$, is assumed for n. For this P_0, the distribution expected in the detector is $P_0^{\rm det}(n_{\rm det}) = \sum_n R(n_{\rm det}, n) P_0(n)$. This is compared to the actual distribution of the raw data, and, making use of Bayes' theorem, an improved multiplicity distribution is calculated, which replaces $P_0(n)$ in the above expression. This process is repeated iteratively until satisfactory agreement between the expected and actual raw data distribution is found. In practice, this occurs after the second iteration if $P_0(n)$ is chosen as the JETSET multiplicity distribution.

The ξ distribution is treated similarly, where n now refers to the bin of the ξ distribution in which a track falls. Further, an extra bin is added to the matrix in order to treat properly tracks which are detected but which arise from processes which on average occur at a distance from the production vertex which is greater than 1 cm, mainly $\rm K^0_S$ and Λ decays, but also secondary interactions and split tracks. For the ξ distributions good agreement is found after five iterations.

In addition, corrections are made for efficiency and acceptance of the event selection, initial state radiation, and $\rm K^0_S$ and Λ decays. Furthermore, the distributions for the b- and light-quark enhanced samples are corrected for the purity of the flavor selection.

Systematic uncertainties

The following sources of systematic uncertainty are investigated:

Selection. The value of each cut used in the event selection is varied independently over a reasonable range and the resulting fully corrected distributions determined. For each multiplicity and ξ-bin, we assign a systematic uncertainty of half of the maximum difference between the new values. The same procedure is followed for the track selection and flavor tagging.

Monte Carlo uncertainties. The analysis is repeated using ARIADNE instead of JETSET to determine the corrections and the unfolding matrix. Further, the b-quark fragmentation parameter, ϵ_b, is varied. Also, the strangeness suppression parameter is varied by an amount consistent with the measured K^0_S production rate [18]. In each case, the difference between the two resulting distributions is taken as the systematic uncertainty.

Unfolding method. Three contributions are determined: First, ARIADNE is used to derive the initial distribution. Secondly, the analysis is repeated using a different number of iterations in the unfolding. Finally, the detector level multiplicity distribution of events generated by ARIADNE is unfolded using the response matrix determined using JETSET events. In each case, the difference is taken as the systematic uncertainty.

The contributions from each of these sources are added in quadrature. The track selection contributes the dominant part of the total systematic uncertainty.

In addition, the accuracy of the simulation of the rate of photon conversion is considered. This is found to be about 15% smaller than in data [11] and is assigned as a systematic uncertainty on $\langle n \rangle$. It is found to be negligible for the other moments. For ξ^* an additional systematic uncertainty is estimated by varying the ξ interval used in the fit. Breakdowns of the systematic uncertainties on $\langle n \rangle$ and ξ^* are shown in Table 1.

	$\langle n \rangle$			ξ^*		
	Sample			Sample		
Source	full	light-q	b-quark	full	light-q	b-quark
Event selection	0.005	0.006	0.004	0.0008	0.0013	0.0006
Track selection	0.090	0.080	0.116	0.0083	0.0084	0.0074
Tagging		0.018	0.021		0.0007	0.0019
MC modelling	0.032	0.031	0.040	0.0040	0.0039	0.0037
Unfolding	0.034	0.034	0.043	0.0018	0.0015	0.0016
γ conversion	0.039	0.039	0.039			
Fit range				0.0147	0.0181	0.0018
Total	0.11	0.10	0.14	0.018	0.020	0.009

Table 1: Contribution of the various sources of systematic uncertainty to the measurement of the mean charged-particle multiplicity, $\langle n \rangle$, and to the peak position (from the Gaussian fit), ξ^*, of the ξ distribution.

Results

ξ distribution

The ξ distribution is measured for all, light-, and b-quark events. Particles coming from K^0_S and Λ decay are included in these spectra. The distributions are shown in Figure 2, where they are compared to the predictions of JETSET and HERWIG. JETSET overestimates the central region. This may be due to the tuning of JETSET, which only uses the charged-particle multiplicity distribution and global event shape data. The description provided by HERWIG is in general poorer, particularly for the b-quark events.

Analytical QCD calculations in the DLLA, assuming LPHD, predict that the ξ distribution is Gaussian. In the MLLA the shape is skewed and flattened [19], which shifts the peak position, ξ^*, to a higher value.

We perform fits to the ξ spectra using both the Gaussian and the Fong-Webber parametrization of the skewed Gaussian [20], which reproduces the expected MLLA shape around the peak value, in the range $2.2 < \xi < 4.8$. This fit range corresponds to using ξ-bins whose content is at least 60% that of the maximum bin. In general, the Fong-Webber parametrization fits better for large values of ξ, while the Gaussian fits better for small values. In the fit region both parametrizations work well except for the b-quark sample. For this sample, the Fong-Webber fit is particularly bad while the Gaussian is acceptable. This may be due to the fact that some particles originate from the b-quark decay rather than from the partonic shower, which would dilute the skewing coming from interference among the gluons in the shower. From the fits we extract the values of ξ^* shown in Table 2.

Sample	Gaussian	Fong-Webber
All	$3.712 \pm 0.008 \pm 0.018$	$3.741 \pm 0.007 \pm 0.011$
Light-quark	$3.743 \pm 0.009 \pm 0.021$	$3.770 \pm 0.008 \pm 0.009$
b-quark	$3.613 \pm 0.007 \pm 0.009$	$3.656 \pm 0.007 \pm 0.026$

Table 2: The peak position, ξ^*, of the ξ distribution from the Gaussian and Fong-Webber fits. The first uncertainty is statistical, the second systematic.

We observe a flavor dependence of ξ^*, more clearly shown by the ratios,

$$\begin{aligned} \xi^*_{\rm light}/\xi^*_{\rm all} &= 1.008 \pm 0.003 \pm 0.001 \\ \xi^*_{\rm b}/\xi^*_{\rm all} &= 0.975 \pm 0.003 \pm 0.004 \quad , \end{aligned}$$

for which much of the systematic uncertainty cancels. Moreover, these ratios are insensitive to the fit parametrization, the small difference being assigned as an additional systematic uncertainty. These values are consistent with the measurements of OPAL [21]. Exclusion of the particles coming from $\rm K^0_S$ and Λ decays shifts the values of ξ^*, but gives consistent values of these ratios [11].

Charged-particle multiplicity distribution

Figure 3 shows the charged-particle multiplicity distribution including $\rm K^0_S$ and Λ decay products for the full, light- and b-quark samples. It is clear that b-quark events tend to have higher multiplicity than light-quark events. All distributions agree rather well with JETSET, but in all cases HERWIG gives a poor description of the data, as is seen in Figures 3a and 3b.

The principal moments of the charged-particle multiplicity distribution are summarized in Table 3. All the moments show significant flavor dependence. However, the flavor dependence of F_2 is quite small. This moment is also quite insensitive to the inclusion or not of $\rm K^0_S$ and Λ decay products.

Furthermore, we find the difference between the mean charged-particle multiplicity of the b-quark sample and that of the light-quark sample to be $2.575 \pm 0.025 \pm 0.054$ when $\rm K^0_S$ and Λ decay products are included and $2.433 \pm 0.025 \pm 0.054$ otherwise.

The H_q are calculated from the charged-particle multiplicity distribution not including $\rm K^0_S$ and Λ decay products. However, they are insensitive to the inclusion of these particles [11].

All events	without K^0_S and Λ decay	with K^0_S and Λ decay
$\langle n \rangle$	$18.63 \pm 0.01 \pm 0.11$	$20.46 \pm 0.01 \pm 0.11$
$D = \sqrt{\langle (n - \langle n \rangle)^2 \rangle}$	$5.888 \pm 0.005 \pm 0.051$	$6.244 \pm 0.005 \pm 0.051$
$S = \langle (n - \langle n \rangle)^3 \rangle / D^3$	$0.596 \pm 0.004 \pm 0.010$	$0.600 \pm 0.004 \pm 0.010$
$K = \langle (n - \langle n \rangle)^4 \rangle / D^4 - 3$	$0.51 \pm 0.01 \pm 0.04$	$0.49 \pm 0.01 \pm 0.03$
$\langle n \rangle / D$	$3.164 \pm 0.002 \pm 0.016$	$3.277 \pm 0.002 \pm 0.016$
$F_2 = \langle n(n-1) \rangle / \langle n \rangle^2$	$1.0461 \pm 0.0002 \pm 0.0040$	$1.0441 \pm 0.0001 \pm 0.0034$
Light-quark events		
$\langle n \rangle$	$18.07 \pm 0.01 \pm 0.10$	$19.88 \pm 0.01 \pm 0.10$
$D = \sqrt{\langle (n - \langle n \rangle)^2 \rangle}$	$5.769 \pm 0.007 \pm 0.054$	$6.111 \pm 0.007 \pm 0.053$
$S = \langle (n - \langle n \rangle)^3 \rangle / D^3$	$0.613 \pm 0.005 \pm 0.013$	$0.617 \pm 0.005 \pm 0.011$
$K = \langle (n - \langle n \rangle)^4 \rangle / D^4 - 3$	$0.54 \pm 0.02 \pm 0.06$	$0.53 \pm 0.02 \pm 0.05$
$\langle n \rangle / D$	$3.133 \pm 0.003 \pm 0.019$	$3.252 \pm 0.003 \pm 0.019$
$F_2 = \langle n(n-1) \rangle / \langle n \rangle^2$	$1.0464 \pm 0.0002 \pm 0.0045$	$1.0441 \pm 0.0002 \pm 0.0038$
b-quark events		
$\langle n \rangle$	$20.51 \pm 0.03 \pm 0.14$	$22.45 \pm 0.03 \pm 0.14$
$D = \sqrt{\langle (n - \langle n \rangle)^2 \rangle}$	$5.78 \pm 0.01 \pm 0.05$	$6.16 \pm 0.01 \pm 0.05$
$S = \langle (n - \langle n \rangle)^3 \rangle / D^3$	$0.574 \pm 0.017 \pm 0.008$	$0.573 \pm 0.017 \pm 0.007$
$K = \langle (n - \langle n \rangle)^4 \rangle / D^4 - 3$	$0.43 \pm 0.04 \pm 0.04$	$0.42 \pm 0.04 \pm 0.03$
$\langle n \rangle / D$	$3.551 \pm 0.006 \pm 0.016$	$3.645 \pm 0.005 \pm 0.015$
$F_2 = \langle n(n-1) \rangle / \langle n \rangle^2$	$1.0305 \pm 0.0003 \pm 0.0027$	$1.0307 \pm 0.0002 \pm 0.0023$

Table 3: Moments of the charged-particle multiplicity distribution for all, light-, and b-quark events. The first uncertainty is statistical, the second systematic.

Since the H_q are sensitive to low statistics at very high multiplicities, it is customary to truncate the multiplicity distribution. The resulting H_q are sensitive to the truncation, which can induce oscillations or increase their size [22]. The truncation also introduces correlations between the H_q, although these are small for low q [11, 22, 23]. Since we want to compare the H_q of various multiplicity distributions, we have to make sure that all distributions are affected by the truncation in the same way. We truncate such that multiplicities with relative error on $P(n)$ greater than 50% are rejected. This corresponds, for all multiplicity distributions studied, to about 0.005% of events. For the full sample, the truncation is at 49.

The H_q for the charged-particle multiplicity distribution from all, light- and b-quark events, shown in Figure 3, have a first negative minimum at $q = 5$ and quasi-oscillations for greater q. They are very similar for the three samples, with only slight differences for the b-quark sample. Similar behavior is seen for JETSET (Figure 3c). Oscillations are also observed for HERWIG (Figure 3d), but they do not agree with those seen in the data.

We also measure the charged-particle multiplicity distributions of 2- and 3-jet events. Events are classified as 2-jet or 3-jet, where the "3-jet" class is the complement of the 2-jet class. The Durham algorithm [24] is applied to calorimeter clusters for values of the jet resolution parameter, $y_{\rm cut}$, ranging from 0.002 to 0.03. The H_q of these multiplicity distributions are also measured. As seen in Figure 4a, there are no oscillations in the $y_{\rm cut} = 0.03$ 3-jet sample but large oscillations in the corresponding 2-jet sample. For $y_{\rm cut} = 0.002$ (Figure 4b), the situation is reversed. The data are well described by JETSET for all $y_{\rm cut}$.

Jet multiplicity distribution

To investigate the origin of the H_q oscillations, we also measure the jet multiplicity distribution. We define jets using the Durham algorithm applied to charged tracks, and thus obtain the number of jets in an event for a particular value of the jet resolution parameter, $y_{\rm cut}$. The energy scale $k_{\rm t}$ of the jets is related to $y_{\rm cut}$ by $k_{\rm t} = \sqrt{s y_{\rm cut}}$. From the distribution of the number of jets per event we calculate the H_q, which are shown in Figure 5 for four different energy scales, representing both non-perturbative and perturbative regions. The corresponding mean jet multiplicity is also given in these figures. We see that JETSET agrees remarkably well with the data, while the agreement of HERWIG is less good, particularly at low $k_{\rm t}$.

Discussion

The pQCD approach

The observed behavior of the H_q is qualitatively similar to that predicted by the NNLLA with the LPHD assumption. However, JETSET also agrees well with all the data samples, even though the parton shower of JETSET does not use the NNLLA. Therefore, we attempt to identify that aspect of the Monte Carlo generator responsible for the agreement. We vary several options in JETSET and study their influence on the behavior of the H_q. First we try several models of parton generation, using in all cases the Lund string fragmentation model: no angular ordering in the parton shower, which makes it essentially a leading log approximation shower with the addition of energy-momentum conservation at each branching; $\mathcal{O}(\alpha_{\rm s})$ and $\mathcal{O}(\alpha_{\rm s}^2)$ matrix elements instead of the parton shower; and the matrix element production of $\rm q\overline{q}$ only. Next, we consider the possibility that this behavior could come from the fragmentation model, which could simulate some hidden higher-order aspects of pQCD. We use JETSET with the above choices of parton generation but with independent fragmentation for the hadronization process.

In all cases, the H_q have a negative first minimum near $q = 5$ and quasi-oscillations for greater q, although the amplitude and the period of the oscillation vary [11]. One might argue that since the JETSET parton shower incorporates energy-momentum conservation at each branching, it is closer to the NNLLA than to the MLLA, and that it is this feature which is the origin of the oscillations [25]. However, we note that oscillations are also produced by JETSET using only the $\rm q\overline{q}$ matrix elements with string fragmentation, or even with independent fragmentation. These models contain no explicit QCD branching at all. Thus we can find oscillatory behavior of the H_q without the NNLLA of pQCD.

Comparison of the H_q of the charged-particle multiplicity distribution with the NNLLA predictions is valid only if the LPHD assumption holds. To remove the dependence on this assumption we investigate the jet multiplicity distribution. This analysis assumes that the jet multiplicity distribution is related to the parton multiplicity distribution at the energy scale corresponding to the jet resolution. By choosing a scale where pQCD is applicable ($\gtrsim 1$ GeV), we can test directly its predictions for the behavior of the H_q.

For $k_{\rm t} = 100$ MeV, the H_q behavior, shown in Figure 5a, is qualitatively similar to that of the charged-particle multiplicity distribution, except that the positions of the minima and maxima are slightly shifted to lower values of q. As $k_{\rm t}$ is increased, the amplitude of the oscillations decreases. A new first minimum appears at $q = 2$, and for $q \leq 5$ the H_q alternate between positive and negative values, as is shown in Figure 5b for $k_{\rm t} = 400$ MeV. For even larger energy scales and in particular in the perturbative region, presented in Figures 5c and 5d

for $k_t \gtrsim 1$ GeV, the oscillations and the negative first minimum near $q = 5$ have completely disappeared. Instead, H_q alternates between positive and negative values for each consecutive value of q with much larger amplitude than in the non-perturbative region. Further, JETSET and, to a lesser extent, HERWIG agree with the data.

The behavior predicted for the H_q by the NNLLA is observed only at very non-perturbative scales. Together with the results of the Monte Carlo studies, this suggests that the minimum and oscillatory behavior of the H_q is not that which is calculated in the NNLLA.

The phenomenological approach

This approach views the charged-particle multiplicity distribution as an average of the corresponding distributions for various processes related to the type of event, *e.g.*, 2-jet, 3-jet, and/or light-quark, heavy-quark events. The multiplicity distribution for each process is assumed to be described by an NBD [8,9], which has no oscillations, while their combination according to Equation 4 might exhibit the oscillatory behavior of the data. We investigate two hypotheses. The first considers the full sample as a mixture of 2- and 3-jet events [8]. We observe that at high values of $y_{\rm cut}$ the 2-jet sample has oscillations and can not be fit by an NBD, while at small values of $y_{\rm cut}$ the oscillations are very small and the NBD fit is good, as has also been observed by DELPHI [26]. For the 3-jet sample the situation is reversed. This behavior is illustrated for the full sample in Figures 4a and 4b. There is no value of $y_{\rm cut}$ for which both the 2-jet and the 3-jet samples are acceptably described by NBDs. Similar behavior is observed restricting the analysis to the light- and b-quark samples.

The second hypothesis considers the full sample as a mixture of light- and b-quark events [9] and is even less successful, also when restricted to the 2-jet and 3-jet samples.

The observation, that low-$y_{\rm cut}$ 2-jet events and high-$y_{\rm cut}$ 3-jet events have no oscillations and are well described by NBDs, suggests the following topology-dependent classification of events:

- "pencil-like" 2-jet events defined by $y_{\rm cut} = 0.004$, about 47% of the events;
- "Mercedes" 3-jet events defined by $y_{\rm cut} = 0.015$, about 28% of the events; and
- "intermediate-jet" events defined as those events not in the other two classifications.

The NBD parametrizations provide reasonable descriptions of all three subsamples, and each subsample is without oscillations, as is shown in Figure 4c. The weighted average of the three NBDs agrees well with the data. The confidence level of the comparison to the multiplicity distribution is 96%, and a reasonable description of the H_q is achieved, as shown in Figure 4d.

Conclusions

The charged-particle multiplicity distribution and the ξ distribution are measured for hadronic Z decays, for all events and for b and non-b events.

The oscillatory behavior observed in the H_q moments of the charged-particle multiplicity distribution does not appear to be related to the NNLLA of pQCD. However, it does appear to be related to the jet topology. Three topologies, each without oscillations, are found: pencil-like 2-jet, Mercedes-like 3-jet, and intermediate topologies. Parametrizing their multiplicity distributions by NBDs, and taking their weighted average results in a good description of both the multiplicity distribution and the H_q of the full sample.

Acknowledgments

We acknowledge useful discussions with I. Dremin, W. Ochs, A. Giovannini and R. Ugoccioni.

References

[1] Ya.I. Azimov *et al.*, Z. Phys. **C 27** (1985) 65; L. Van Hove and A. Giovannini, Acta Phys. Pol. **B 19** (1988) 917.

[2] E.A. De Wolf, I.M. Dremin and W. Kittel, Phys. Rep. **270** (1996) 1.

[3] I.M. Dremin, Physics-Uspekhi **37** (1994) 715.

[4] I.M. Dremin *et al.*, Phys. Lett. **B 336** (1994) 119; N. Nakajima, M. Biyajima and N. Suzuki, Phys. Rev. **D 54** (1996) 4333; SLD Collab., K. Abe *et al.*, Phys. Lett. **B 371** (1996) 149; Wang Shaoshun *et al.*, Phys. Rev. **D 56** (1997) 1668; A. Capella *et al.*, Z. Phys. **C 75** (1997) 89; I.M. Dremin *et al.*, Phys. Lett. **B 403** (1997) 149.

[5] I.M. Dremin, Phys. Lett. **B 313** (1993) 209; I.M. Dremin and V.A. Nechitaĭlo, JETP Lett. **58** (1993) 881.

[6] Norbert Schmitz, *Multiparticle Dynamics*, eds. A. Giovannini and W. Kittel (World Scientific, Singapore, 1990) p. 25; Alberto Giovannini, *Proc. XXVI Int. Symposium on Multiparticle Dynamics*, eds. J. Dias de Deus *et al.* (World Scientific, Singapore, 1997) p. 232; HRS Collab., M. Derrick *et al.*, Phys. Rev. **D 34** (1986) 3304; TASSO Collab., W. Braunschweig *et al.*, Z. Phys. **C 45** (1989) 193.

[7] DELPHI Collab., P. Abreu *et al.*, Z. Phys. **C 50** (1991) 185.

[8] A. Giovannini, S. Lupia and R. Ugoccioni, Phys. Lett. **B 374** (1996) 231.

[9] A. Giovannini, S. Lupia and R. Ugoccioni, Phys. Lett. **B 388** (1996) 639.

[10] L3 Collab., B. Adeva *et al.*, Nucl. Instr. Meth. **A 289** (1990) 35;
J.A. Bakken *et al.*, Nucl. Instr. Meth. **A 275** (1989) 81;
O. Adriani *et al.*, Nucl. Instr. Meth. **A 302** (1991) 53;
B. Adeva *et al.*, Nucl. Instr. Meth. **A 323** (1992) 109;
K. Deiters *et al.*, Nucl. Instr. Meth. **A 323** (1992) 162;
M. Acciari *et al.*, Nucl. Instr. Meth. **A 351** (1994) 300.

[11] D. J. Mangeol, Ph.D. thesis, Univ. of Nijmegen, 2002.

[12] T. Sjöstrand, Comp. Phys. Comm. **82** (1994) 74.

[13] The L3 detector simulation is based on GEANT, see R. Brun *et al.*, report CERN DD/EE/84-1 (1984), revised 1987, and uses GHEISHA to simulate hadronic interactions, see H. Fesefeldt, RWTH Aachen report PITHA 85/02 (1985).

[14] L. Lönnblad, Comp. Phys. Comm. **71** (1992) 15.

[15] G. Marchesini *et al.*, Comp. Phys. Comm. **67** (1992) 465.

[16] L3 Collab., M. Acciarri *et al.*, Phys. Lett. **B 411** (1997) 373.

[17] G. D'Agostini, Nucl. Inst. Meth. **A 362** (1995) 487.

[18] Particle Data Group, D. E. Groom *et al.*, Eur. Phys. J. **C 15** (2000) 1.

[19] Yu. Dokshitzer *et al.*, *Basics of Perturbative QCD*, (Editions Frontières, Gif-sur-Yvette, 1991).

[20] C.P. Fong and B.R. Webber, Phys. Lett. **B 229** (1989) 289.

[21] OPAL Collab., K. Ackerstaff *et al.*, E. Phys. J. **C 7** (1999) 369.

[22] A. Giovannini, S. Lupia and R. Ugoccioni, Phys. Lett. **B 342** (1995) 387.

[23] OPAL Collab., K. Ackerstaff *et al.*, E. Phys. J. **C 1** (1998) 479.

[24] S. Bethke *et al.*, Nucl. Phys. **B 370** (1992) 310.

[25] I.M. Dremin and J.W. Gary, Phys. Rep. **349** (2001) 301.

[26] DELPHI Collab., P. Abreu *et al.*, Z. Phys. **C 56** (1992) 63.

Author List

The L3 Collaboration:

P.Achard,[20] O.Adriani,[17] M.Aguilar-Benitez,[24] J.Alcaraz,[24,18] G.Alemanni,[22] J.Allaby,[18] A.Aloisio,[28] M.G.Alviggi,[28] H.Anderhub,[47] V.P.Andreev,[6,33] F.Anselmo,[9] A.Arefiev,[27] T.Azemoon,[3] T.Aziz,[10,18] P.Bagnaia,[38] A.Bajo,[24] G.Baksay,[16] L.Baksay,[25] S.V.Baldew,[2] S.Banerjee,[10] Sw.Banerjee,[4] A.Barczyk,[47,45] R.Barillère,[18] P.Bartalini,[22] M.Basile,[9] N.Batalova,[44] R.Battiston,[32] A.Bay,[22] F.Becattini,[17] U.Becker,[14] F.Behner,[47] L.Bellucci,[17] R.Berbeco,[3] J.Berdugo,[24] P.Berges,[14] B.Bertucci,[32] B.L.Betev,[47] M.Biasini,[32] M.Biglietti,[28] A.Biland,[47] J.J.Blaising,[4] S.C.Blyth,[34] G.J.Bobbink,[2] A.Böhm,[1] L.Boldizsar,[13] B.Borgia,[38] S.Bottai,[17] D.Bourilkov,[47] M.Bourquin,[20] S.Braccini,[20] J.G.Branson,[40] F.Brochu,[4] A.Buijs,[43] J.D.Burger,[14] W.J.Burger,[32] X.D.Cai,[14] M.Capell,[14] G.Cara Romeo,[9] G.Carlino,[28] A.Cartacci,[17] J.Casaus,[24] F.Cavallari,[38] N.Cavallo,[35] C.Cecchi,[32] M.Cerrada,[24] M.Chamizo,[20] Y.H.Chang,[49] M.Chemarin,[23] A.Chen,[49] G.Chen,[7] G.M.Chen,[7] H.F.Chen,[21] H.S.Chen,[7] G.Chiefari,[28] L.Cifarelli,[39] F.Cindolo,[9] I.Clare,[14] R.Clare,[37] G.Coignet,[4] N.Colino,[24] S.Costantini,[38] B.de la Cruz,[24] S.Cucciarelli,[32] J.A.van Dalen,[30] R.de Asmundis,[28] P.Déglon,[20] J.Debreczeni,[13] A.Degré,[4] K.Deiters,[45] D.della Volpe,[28] E.Delmeire,[20] P.Denes,[36] F.DeNotaristefani,[38] A.De Salvo,[47] M.Diemoz,[38] M.Dierckxsens,[2] D.van Dierendonck,[2] C.Dionisi,[38] M.Dittmar,[47,18] A.Doria,[28] M.T.Dova,[11,♯] D.Duchesneau,[4] P.Duinker,[2] B.Echenard,[20] A.Eline,[18] H.El Mamouni,[23] A.Engler,[34] F.J.Eppling,[14] A.Ewers,[1] P.Extermann,[20] M.A.Falagan,[24] S.Falciano,[38] A.Favara,[31] J.Fay,[23] O.Fedin,[33] M.Felcini,[47] T.Ferguson,[34] H.Fesefeldt,[1] E.Fiandrini,[32] J.H.Field,[20] F.Filthaut,[30] P.H.Fisher,[14] W.Fisher,[36] I.Fisk,[40] G.Forconi,[14] K.Freudenreich,[47] C.Furetta,[26] Yu.Galaktionov,[27,14] S.N.Ganguli,[10] P.Garcia-Abia,[5,18] M.Gataullin,[31] S.Gentile,[38] S.Giagu,[38] Z.F.Gong,[21] G.Grenier,[23] O.Grimm,[47] M.W.Gruenewald,[8,1] M.Guida,[39] R.van Gulik,[2] V.K.Gupta,[36] A.Gurtu,[10] L.J.Gutay,[44] D.Haas,[5] D.Hatzifotiadou,[9] T.Hebbeker,[8,1] A.Hervé,[18] J.Hirschfelder,[34] H.Hofer,[47] M.Hohlmann,[25] G.Holzner,[47] S.R.Hou,[49] Y.Hu,[30] B.N.Jin,[7] L.W.Jones,[3] P.de Jong,[2] I.Josa-Mutuberría,[24] D.Käfer,[1] M.Kaur,[15] M.N.Kienzle-Focacci,[20] J.K.Kim,[42] J.Kirkby,[18] W.Kittel,[30] A.Klimentov,[14,27] A.C.König,[30] M.Kopal,[44] V.Koutsenko,[14,27] M.Kräber,[47] R.W.Kraemer,[34] W.Krenz,[1] A.Krüger,[46] A.Kunin,[14] P.Ladron de Guevara,[24] I.Laktineh,[23] G.Landi,[17] M.Lebeau,[18] A.Lebedev,[14] P.Lebrun,[23] P.Lecomte,[47] P.Lecoq,[18] P.Le Coultre,[47] J.M.Le Goff,[18] R.Leiste,[46] P.Levtchenko,[33] C.Li,[21] S.Likhoded,[46] C.H.Lin,[49] W.T.Lin,[49] F.L.Linde,[2] L.Lista,[28] Z.A.Liu,[7] W.Lohmann,[46] E.Longo,[38] Y.S.Lu,[7] K.Lübelsmeyer,[1] C.Luci,[38] L.Luminari,[38] W.Lustermann,[47] W.G.Ma,[21] L.Malgeri,[20] A.Malinin,[27] C.Maña,[24] D.Mangeol,[30] J.Mans,[36] J.P.Martin,[23] F.Marzano,[38] K.Mazumdar,[10] R.R.McNeil,[6] S.Mele,[18,28] L.Merola,[28] M.Meschini,[17] W.J.Metzger,[30] A.Mihul,[12] H.Milcent,[18] G.Mirabelli,[38] J.Mnich,[1] G.B.Mohanty,[10] G.S.Muanza,[23] A.J.M.Muijs,[2] B.Musicar,[40] M.Musy,[38] S.Nagy,[16] S.Natale,[20] M.Napolitano,[28] F.Nessi-Tedaldi,[47] H.Newman,[31] T.Niessen,[1] A.Nisati,[38] H.Nowak,[46] R.Ofierzynski,[47] G.Organtini,[38] C.Palomares,[18] D.Pandoulas,[1] P.Paolucci,[28] R.Paramatti,[38] G.Passaleva,[17] S.Patricelli,[28] T.Paul,[11] M.Pauluzzi,[32] C.Paus,[14] F.Pauss,[47] M.Pedace,[38] S.Pensotti,[26] D.Perret-Gallix,[4] B.Petersen,[30] D.Piccolo,[28] F.Pierella,[9] M.Pioppi,[32] P.A.Piroué,[36] E.Pistolesi,[26] V.Plyaskin,[27] M.Pohl,[20] V.Pojidaev,[17] J.Pothier,[18] D.O.Prokofiev,[44] D.Prokofiev,[33] J.Quartieri,[39] G.Rahal-Callot,[47] M.A.Rahaman,[10] P.Raics,[16] N.Raja,[10] R.Ramelli,[47] P.G.Rancoita,[26] R.Ranieri,[17] A.Raspereza,[46] P.Razis,[29] D.Ren,[47] M.Rescigno,[38] S.Reucroft,[11] S.Riemann,[46] K.Riles,[3] B.P.Roe,[3] L.Romero,[24] A.Rosca,[8] S.Rosier-Lees,[4] S.Roth,[1] C.Rosenbleck,[1] B.Roux,[30] J.A.Rubio,[18] G.Ruggiero,[17] H.Rykaczewski,[47] A.Sakharov,[47] S.Saremi,[6] S.Sarkar,[38] J.Salicio,[18] E.Sanchez,[24] M.P.Sanders,[30] C.Schäfer,[18] V.Schegelsky,[33] S.Schmidt-Kaerst,[1] D.Schmitz,[1] H.Schopper,[48] D.J.Schotanus,[30] G.Schwering,[1] C.Sciacca,[28] L.Servoli,[32] S.Shevchenko,[31] N.Shivarov,[41] V.Shoutko,[14] E.Shumilov,[27] A.Shvorob,[31] T.Siedenburg,[1] D.Son,[42] P.Spillantini,[17] M.Steuer,[14] D.P.Stickland,[36] B.Stoyanov,[41] A.Straessner,[18] K.Sudhakar,[10] G.Sultanov,[41] L.Z.Sun,[21] S.Sushkov,[8] H.Suter,[47] J.D.Swain,[11] Z.Szillasi,[25,¶] X.W.Tang,[7] P.Tarjan,[16] L.Tauscher,[5] L.Taylor,[11] B.Tellili,[23] D.Teyssier,[23] C.Timmermans,[30] Samuel C.C.Ting,[14] S.M.Ting,[14] S.C.Tonwar,[10,18] J.Tóth,[13] C.Tully,[36] K.L.Tung,[7] J.Ulbricht,[47] E.Valente,[38] R.T.Van de Walle,[30] V.Veszpremi,[25] G.Vesztergombi,[13] I.Vetlitsky,[27] D.Vicinanza,[39] G.Viertel,[47] S.Villa,[37] M.Vivargent,[4] S.Vlachos,[5] I.Vodopianov,[33] H.Vogel,[34] H.Vogt,[46] I.Vorobiev,[3427] A.A.Vorobyov,[33] M.Wadhwa,[5] W.Wallraff,[1] X.L.Wang,[21] Z.M.Wang,[21] M.Weber,[1] P.Wienemann,[1] H.Wilkens,[30] S.Wynhoff,[36] L.Xia,[31] Z.Z.Xu,[21] J.Yamamoto,[3] B.Z.Yang,[21] C.G.Yang,[7] H.J.Yang,[3] M.Yang,[7] S.C.Yeh,[50] An.Zalite,[33] Yu.Zalite,[33] Z.P.Zhang,[21] J.Zhao,[21] G.Y.Zhu,[7] R.Y.Zhu,[31] H.L.Zhuang,[7] A.Zichichi,[9,18,19] G.Zilizi,[25,¶] B.Zimmermann,[47] M.Zöller.[1]

1 I. Physikalisches Institut, RWTH, D-52056 Aachen, FRG[§]
III. Physikalisches Institut, RWTH, D-52056 Aachen, FRG[§]
2 National Institute for High Energy Physics, NIKHEF, and University of Amsterdam, NL-1009 DB Amsterdam, The Netherlands
3 University of Michigan, Ann Arbor, MI 48109, USA
4 Laboratoire d'Annecy-le-Vieux de Physique des Particules, LAPP,IN2P3-CNRS, BP 110, F-74941 Annecy-le-Vieux CEDEX, France
5 Institute of Physics, University of Basel, CH-4056 Basel, Switzerland
6 Louisiana State University, Baton Rouge, LA 70803, USA
7 Institute of High Energy Physics, IHEP, 100039 Beijing, China[△]
8 Humboldt University, D-10099 Berlin, FRG[§]
9 University of Bologna and INFN-Sezione di Bologna, I-40126 Bologna, Italy
10 Tata Institute of Fundamental Research, Mumbai (Bombay) 400 005, India
11 Northeastern University, Boston, MA 02115, USA
12 Institute of Atomic Physics and University of Bucharest, R-76900 Bucharest, Romania
13 Central Research Institute for Physics of the Hungarian Academy of Sciences, H-1525 Budapest 114, Hungary[‡]
14 Massachusetts Institute of Technology, Cambridge, MA 02139, USA
15 Panjab University, Chandigarh 160 014, India.
16 KLTE-ATOMKI, H-4010 Debrecen, Hungary[¶]
17 INFN Sezione di Firenze and University of Florence, I-50125 Florence, Italy
18 European Laboratory for Particle Physics, CERN, CH-1211 Geneva 23, Switzerland
19 World Laboratory, FBLJA Project, CH-1211 Geneva 23, Switzerland
20 University of Geneva, CH-1211 Geneva 4, Switzerland
21 Chinese University of Science and Technology, USTC, Hefei, Anhui 230 029, China[△]
22 University of Lausanne, CH-1015 Lausanne, Switzerland
23 Institut de Physique Nucléaire de Lyon, IN2P3-CNRS,Université Claude Bernard, F-69622 Villeurbanne, France
24 Centro de Investigaciones Energéticas, Medioambientales y Tecnológicas, CIEMAT, E-28040 Madrid, Spain[♭]
25 Florida Institute of Technology, Melbourne, FL 32901, USA
26 INFN-Sezione di Milano, I-20133 Milan, Italy
27 Institute of Theoretical and Experimental Physics, ITEP, Moscow, Russia
28 INFN-Sezione di Napoli and University of Naples, I-80125 Naples, Italy
29 Department of Physics, University of Cyprus, Nicosia, Cyprus
30 University of Nijmegen and NIKHEF, NL-6525 ED Nijmegen, The Netherlands
31 California Institute of Technology, Pasadena, CA 91125, USA
32 INFN-Sezione di Perugia and Università Degli Studi di Perugia, I-06100 Perugia, Italy
33 Nuclear Physics Institute, St. Petersburg, Russia
34 Carnegie Mellon University, Pittsburgh, PA 15213, USA
35 INFN-Sezione di Napoli and University of Potenza, I-85100 Potenza, Italy
36 Princeton University, Princeton, NJ 08544, USA
37 University of Californa, Riverside, CA 92521, USA
38 INFN-Sezione di Roma and University of Rome, "La Sapienza", I-00185 Rome, Italy
39 University and INFN, Salerno, I-84100 Salerno, Italy
40 University of California, San Diego, CA 92093, USA
41 Bulgarian Academy of Sciences, Central Lab. of Mechatronics and Instrumentation, BU-1113 Sofia, Bulgaria
42 The Center for High Energy Physics, Kyungpook National University, 702-701 Taegu, Republic of Korea
43 Utrecht University and NIKHEF, NL-3584 CB Utrecht, The Netherlands
44 Purdue University, West Lafayette, IN 47907, USA
45 Paul Scherrer Institut, PSI, CH-5232 Villigen, Switzerland
46 DESY, D-15738 Zeuthen, FRG
47 Eidgenössische Technische Hochschule, ETH Zürich, CH-8093 Zürich, Switzerland
48 University of Hamburg, D-22761 Hamburg, FRG
49 National Central University, Chung-Li, Taiwan, China
50 Department of Physics, National Tsing Hua University, Taiwan, China
§ Supported by the German Bundesministerium für Bildung, Wissenschaft, Forschung und Technologie
‡ Supported by the Hungarian OTKA fund under contract numbers T019181, F023259 and T024011.
¶ Also supported by the Hungarian OTKA fund under contract number T026178.
♭ Supported also by the Comisión Interministerial de Ciencia y Tecnología.
♯ Also supported by CONICET and Universidad Nacional de La Plata, CC 67, 1900 La Plata, Argentina.
△ Supported by the National Natural Science Foundation of China.

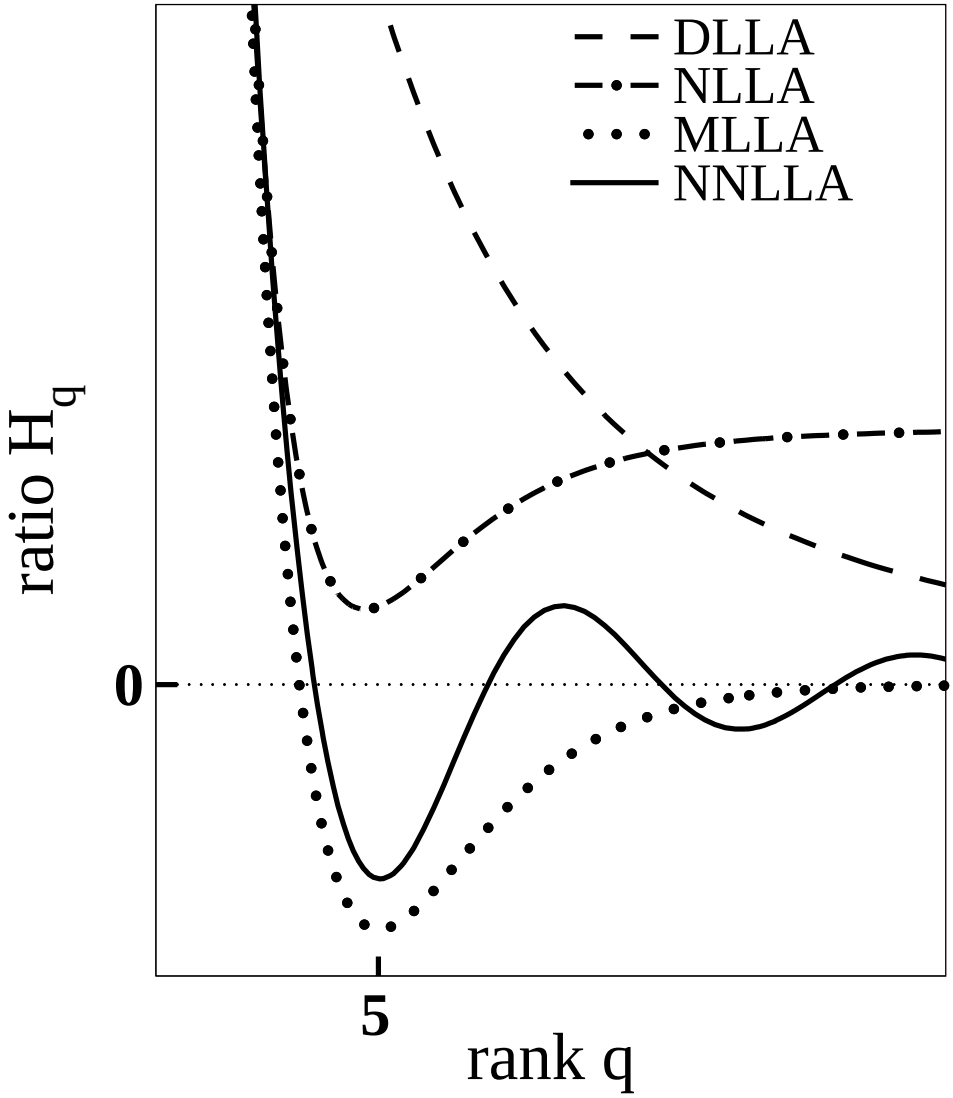

Figure 1: Qualitative behavior of H_q as a function of q for various approximations of perturbative QCD [3,5].

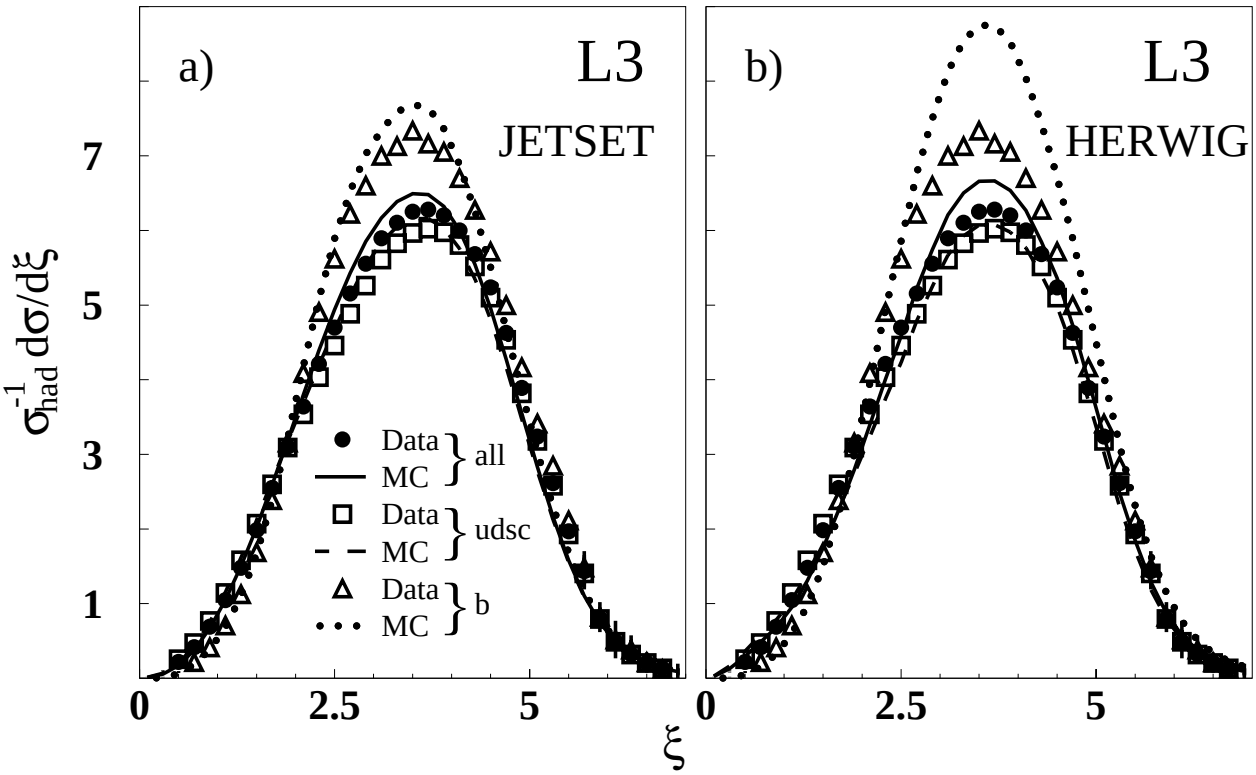

Figure 2: Distribution of $\xi = \ln(\sqrt{s}/2p)$ for b-quark, light-quark and all events compared to the expectations of (a) JETSET and (b) HERWIG. $\sigma_{\rm had}$ is the hadronic cross section.

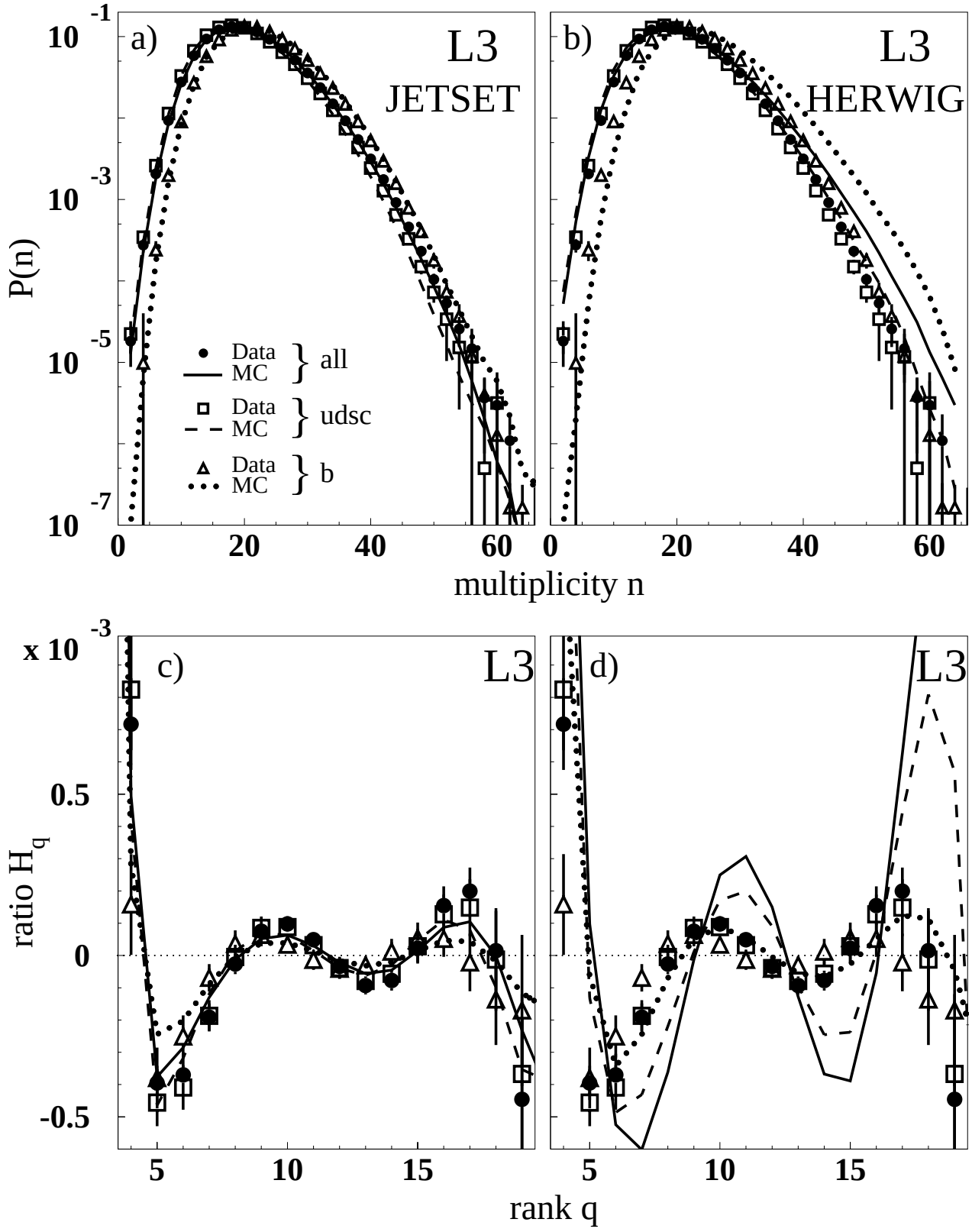

Figure 3: Charged-particle multiplicity distribution for all, light-, and b-quark events compared to the expectations of (a) JETSET and (b) HERWIG, and the H_q compared to the expectations of (c) JETSET and (d) HERWIG.

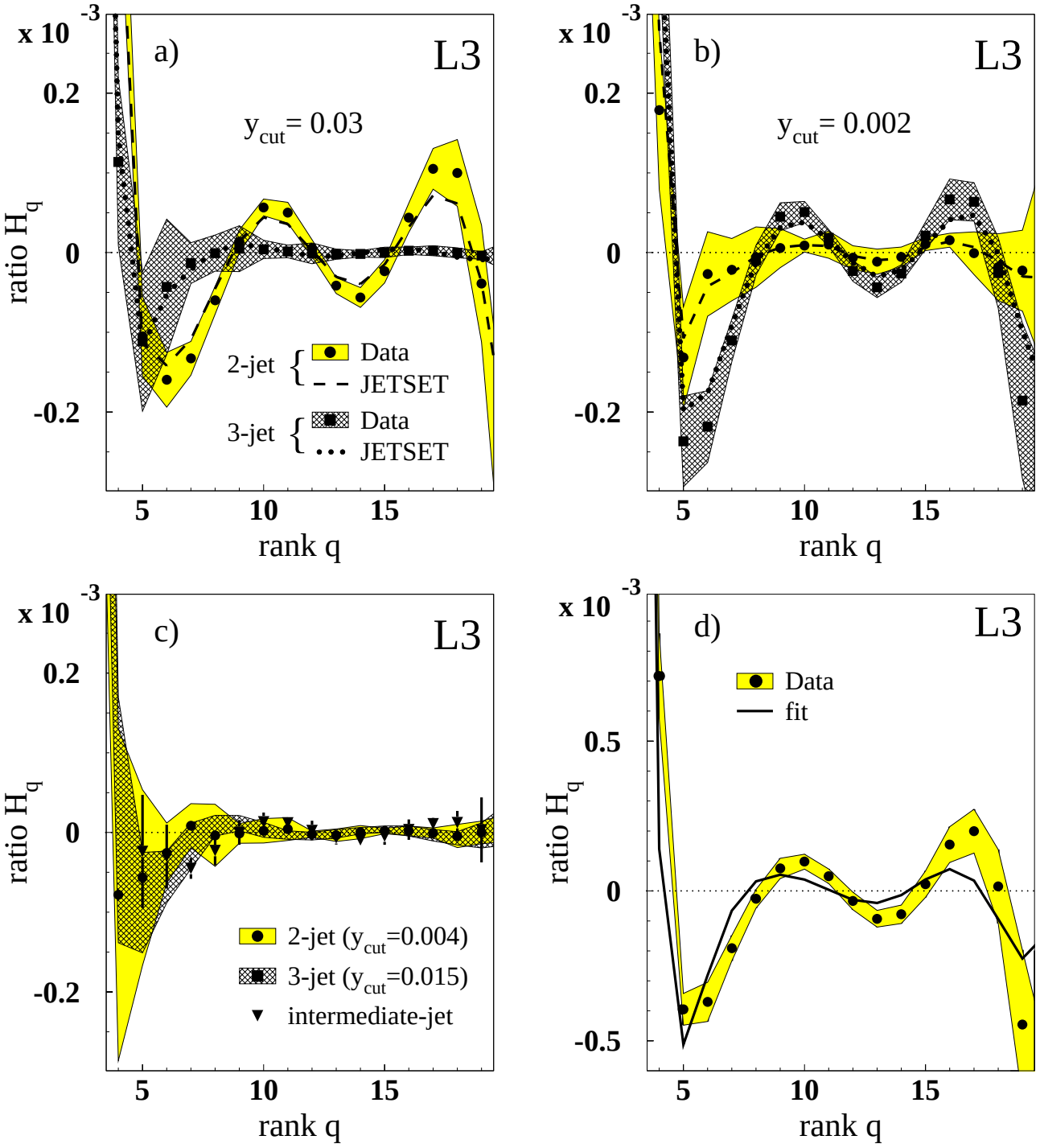

Figure 4: H_q of the charged-particle multiplicity distribution, for all flavors, of the 2-jet and 3-jet events obtained with (a) $y_{\rm cut} = 0.03$, (b) $y_{\rm cut} = 0.002$, (c) for the 2-jet sample with $y_{\rm cut} = 0.004$, the 3-jet sample with $y_{\rm cut} = 0.015$, and the "intermediate-jet" sample, and (d) for all events. Also shown in (d) are the result of the NBD parametrizations of the three samples of (c).

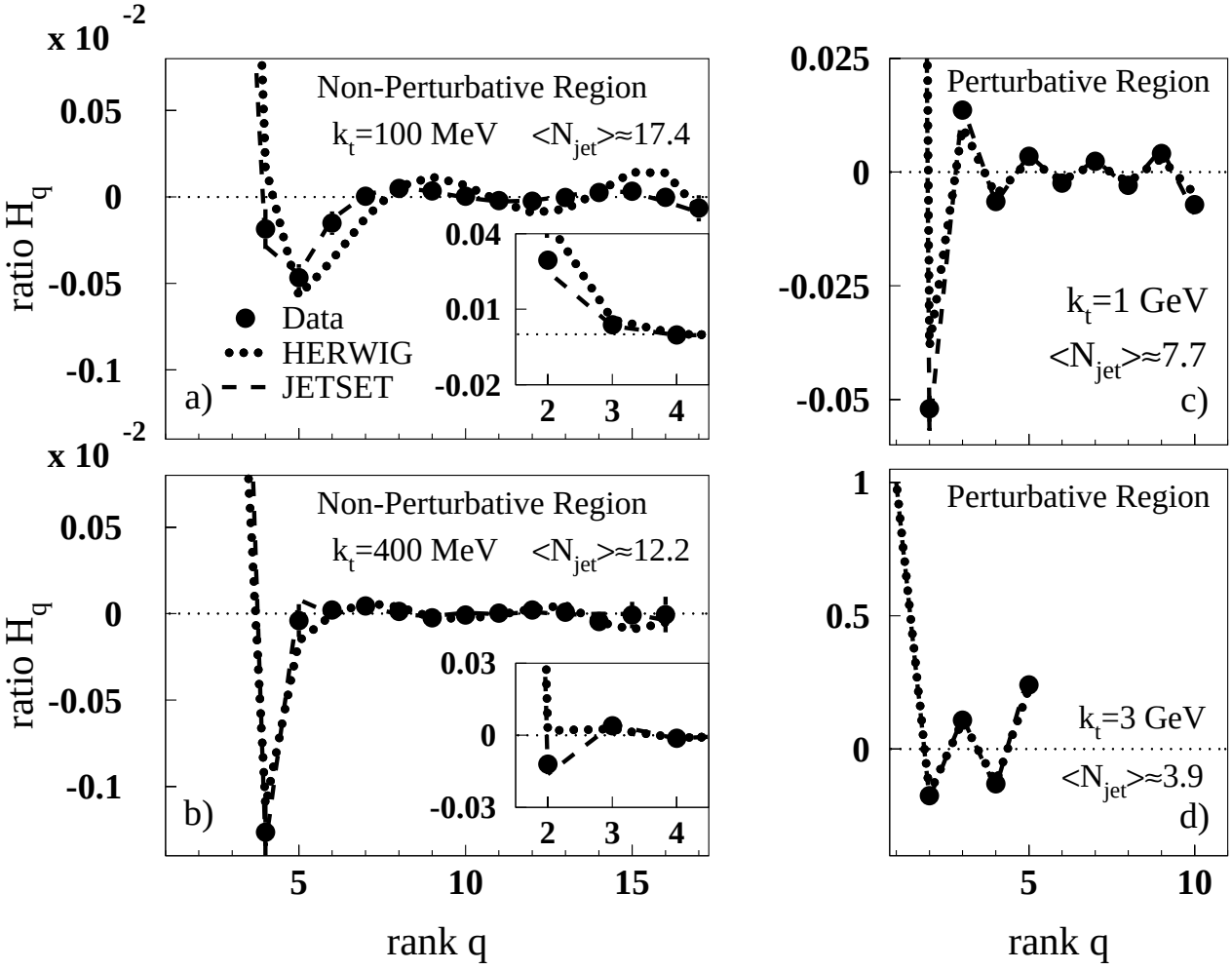

Figure 5: H_q of the jet multiplicity distributions at non-perturbative energy scales, (a) $k_{\mathrm{t}} = 100$ MeV and (b) $k_{\mathrm{t}} = 400$ MeV, and at perturbative energy scales, (c) $k_{\mathrm{t}} = 1$ GeV and (d) $k_{\mathrm{t}} = 3$ GeV. The inserts show the low-q points, most of which lie outside the main plots. Also indicated are the corresponding mean jet multiplicities. The data are compared to JETSET and HERWIG.